Skeletal Radiology (2019) 48:1011–1021
https://doi.org/10.1007/s00256-019-3160-4

REVIEW ARTICLE

Magnetic resonance imaging of subchondral insufficiency fractures of the lower limb

Sangoh Lee[1,2] · Asif Saifuddin[2,3]

Received: 15 October 2018 / Revised: 4 December 2018 / Accepted: 10 January 2019 / Published online: 31 January 2019

Abstract

Subchondral insufficiency fracture (SIF) is a non-traumatic condition that has historically been associated with elderly, osteoporotic women and patients with systemic conditions. There has been much work done to determine the pathogenesis of SIF, which has previously been regarded as idiopathic, rapid-progressive osteoarthritis or osteonecrosis of the hip, spontaneous osteonecrosis of the knee (SONK), osteochondral defect (OCD) of the talus and adult-onset Freiberg infraction of the metatarsal head. Early diagnosis and management are crucial to prevent subchondral collapse, secondary osteonecrosis and early-onset osteoarthritis. Magnetic resonance imaging (MRI) plays an important role in the diagnosis of SIF, which is often inconspicuous on initial radiographs. In this article, the authors provide an update on the role of MRI in identifying key imaging features of SIF in various joints of the lower limb to aid in its correct diagnosis.

Keywords Subchondral insufficiency fracture · Hip · Knee · Ankle · Metatarsal · Lower limb · Magnetic resonance imaging

Introduction

Subchondral insufficiency fracture (SIF) is a condition that may not be associated with a clear history of trauma or may be related to repetitive microtrauma, and occurs immediately below the articular cartilage of a weight-bearing joint. Initially described by Bangil et al. in 1996, it was thought to occur secondary to physiological stress applied to a weakened bone due to reduced bone mineralisation, commonly seen in post-menopausal, osteoporotic women [1]. Cases of SIF have also been seen in patients with rheumatoid arthritis, and those who have undergone liver and renal transplantation [2–4]. However, subsequent literature has found that although patients usually have concurrent osteopaenia, it is not thought to be the cause of SIF [5, 6]. In fact, Nelson et al. showed that 43% of patients had normal T score (bone mineral density when compared with a young normal reference mean), and the average Z score (age-matched reference mean) was nearly one standard deviation above normal [6]. It is hypothesised that cartilage and meniscal degeneration might promote a specific metabolic response that leads to SIF in this group of patients [6].

Prognosis is highly variable and depends on age, weight, bone density and extent of the fracture [7]. Conservative management includes non-weight-bearing initially, followed by gradual load-bearing as tolerated by the patient. Concurrent use of cold therapy, non-steroidal anti-inflammatory drugs (NSAIDs) and crutches is the mainstay of conservative therapy [8, 9]. However, as initial radiographs are normal in most cases, there is a tendency for delayed diagnosis and suboptimal early management that may result in worsened outcome owing to subchondral collapse, potentially requiring surgery [10].

It is important to note that although SIF and osteonecrosis (ON) can occur at similar anatomical locations, they have different histopathological and radiological appearances [11, 12]. Treatment for the two conditions is also different; therefore, it is important to be able to correctly identify and differentiate the two conditions on imaging. The magnetic resonance imaging (MRI) features of SIF at various locations have been previously described [13]. This review article provides an update on the role of MRI in the diagnosis and management

✉ Sangoh Lee
sangoh.lee@nhs.net

[1] Department of Clinical Imaging, Imperial College Healthcare NHS Trust, London, UK

[2] Royal National Orthopaedic Hospital NHS Trust, Stanmore, UK

[3] Everlight Radiology, Level 6, West, 350 Euston Rd, London, UK

of SIF in the various joints of the lower limb, highlighting key findings that aid its correct diagnosis.

Anatomy of the subchondral bone plate

The anatomy of the subchondral bone is complex and is different from that seen on a non-articular bone surface. It consists of two mineralised layers that separate the articular cartilage from the underlying bone marrow. The first layer is formed by calcified cartilage, which is radiologically denser than the adjacent articular cartilage. There is a smooth transition between the two cartilage layers, which is organised in a complex three-dimensional trilaminate structure [14, 15]. This layer of transition is known as the "tidemark" because of its characteristic appearance on histological sections (Fig. 1) [15]. The tidemark is thought to have an important biomechanical function and is seen to advance into the uncalcified articular cartilage in the presence of microtrauma [16]. From the tidemark to the underlying bone marrow, the calcified cartilage transitions into a woven or lamellar bone that is formed in a perpendicular direction to the joint surface, with a further cross-network of finer trabeculae that are formed in a right-angle orientation [17]. Importantly, no continuous collagen fibres are seen between the calcified cartilage layer and the subchondral bone plate, thus representing a zone of weakness at the osteochondral junction [17]. There is a marked difference in the rigidity and the ability to withstand shear forces from the articular cartilage to the subchondral bone, and this is thought to be the reason why there is a propensity for cartilage injury secondary to shear forces [18].

Function

The subchondral bone plate has an important function in providing support to the overlying articular cartilage. Both articular cartilage and the subchondral bone are thought to act as a dynamic unit that dissipates mechanical forces exerted on the diarthrodial joint [18, 19]. Therefore, it is thought that osteoarthritis (OA) is not a disease of the articular cartilage alone, and any anatomical alterations will result in reciprocal changes in the mechanical properties of the other [17, 20]. Joint congruency, defined as a measurement of two opposing joint surfaces that are in contact with one another, is regarded as an important factor in determining the thickness of the articular cartilage [21]. Joints with regions of high congruency appear to have thinner articular cartilage, whereas joints with regions of low congruency appear to have thicker articular cartilage [22]. For example, the ankle has thin articular cartilage measuring 1.2 mm (1.0–1.6) with a high joint congruency ratio (average length of the congruent surface divided by the average length of the total articular surface), whereas the knee has thick articular cartilage measuring 2.2 mm (1.7–2.6) with a low joint congruency ratio. Joints with high congruency have a large surface area to dissipate the mechanical load, and therefore do not require thick articular cartilage. Conversely, joints with low congruency require thick articular cartilage that can easily be deformed to provide a larger surface area, thereby decreasing the stress per unit area [22]. This would support the hypothesis that OA might play an important role in the pathophysiology of SIF. Cartilage and meniscal degeneration lead to an altered biomechanical state, causing increased stress to be exerted on the weight-bearing aspect of the joint [21–23]. Therefore, it would no longer dissipate the mechanical force

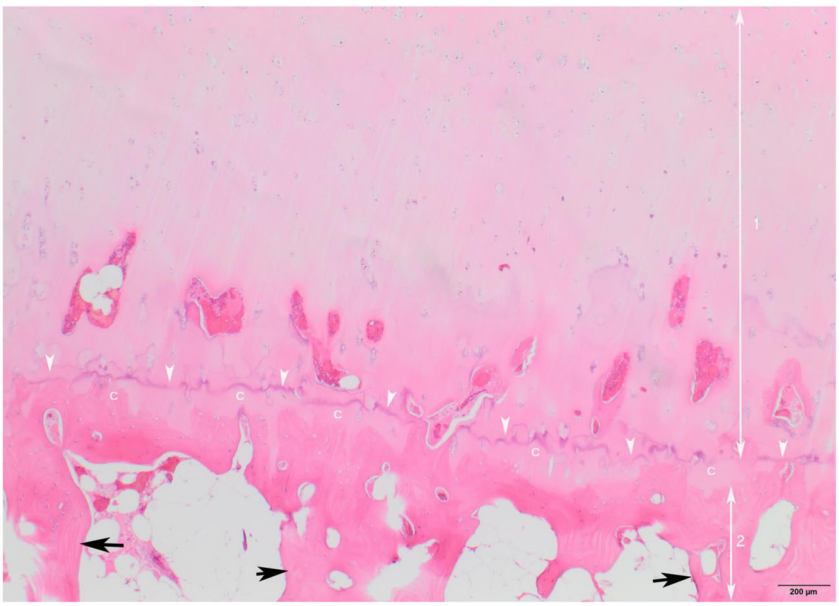

Fig. 1 Anatomy of the articular surface of the femoral head (H & E; magnification ×200). Zone 1 represents the hyaline cartilage, which is separated from the calcified cartilage (C) by the "tidemark" (*arrowheads*). Zone 2 represents the subchondral bone containing trabeculae orientated perpendicular to the articular surface (*black arrows*)

uniformly across the joint, resulting in SIF notably along the anterosuperior margin of the femoral head, the medial femoral condyle and the talar dome.

Hips

Subchondral insufficiency fracture and ON are known causes of femoral head collapse. A study by Yamamoto et al. found that 6.5% of femoral heads surgically resected, with a clinical diagnosis of either OA or ON, had SIF on histopathological analysis [11]. The age range of these patients was 20–93 years with a mean age of 68 years, 79% of patients being over 60 years of age and 60.1% being female. In a further study, 10 hips with confirmed SIF had callus with granulation tissue along either edge of the fracture line, suggestive of a potential for the fracture to heal [7]. It is important to differentiate SIF from ON as early diagnosis would have an impact on the treatment and its overall management, the prognosis depending on initial treatment, weight, activity, degree of osteopaenia and extent of the fracture. A study by Yoon et al. found that 41.9% of SIF cases (13 out of 31) had femoral head collapse along the anterosuperior margin, with a further 3 cases progressing to femoral head collapse on follow-up radiographs. Of these, 48.4% (15 out of 31) underwent total hip arthroplasty (THA) due to failure of conservative therapy [24].

Initial hip radiographs in patients with SIF are generally normal (Fig. 2a) and inconsistent with the severity of the pain. Repeat radiography several months later may demonstrate subchondral sclerosis due to callus formation, or femoral head collapse in those with fracture progression. In these individuals, a "crescent sign" or femoral head deformity is evident [7]. MRI demonstrates a pattern of bone marrow oedema (BMO) with a focal low signal intensity (SI) band on T1-weighted (T1W) imaging (Fig. 2b, c) [7, 9, 11]. Although this is a finding seen in both ON and SIF, two distinct features have been identified that can help differentiate the two conditions. In SIF, the bone segment between the articular cartilage and low SI band shows high SI on T2-weighted and gadolinium-enhanced images, whereas it does not in ON, as this segment of bone is deemed necrotic (Fig. 3a). The shape of the low SI band in SIF typically parallels the articular surface and is often discontinuous, with a serpentine morphology (Fig. 3b). In ON, the low SI band is usually smooth, concave and continuous (Fig. 3c) [7, 11, 25, 26]. The appearance of the subchondral bone directly above the low SI T1 band on fat-suppressed T2-weighted (T2W) MR images in SIF has been divided into three types, which may relate to outcome [27]. Type 1 (52.5%) showed high SI, type 2 (20%) showed heterogeneous SI (Fig. 4) and type 3 (27.5%) showed low SI. Of these, healing rates were 86% and 75% for type 1 and 2 hips respectively, but only 18% for type 3 hips. Also, the location of BMO may predict clinical outcome. In a study of 15 hips diagnosed with SIF, BMO was seen in the femoral head in only 6 (Figs. 2c, 3b), in the acetabulum alone in 2 and in both the femoral head and the acetabulum in 7 cases [28]. Of the 7 patients with BMO on both sides of the joint, 3 progressed to rapidly destructive arthrosis, whereas most patients with BMO limited to one side of the joint were successfully treated using conservative measures.

However, a further study by Yamamoto et al. found that there was considerable variation in the image findings, making definitive diagnosis difficult with MRI alone [29]. Secondary subchondral bone fracture in the presence of ON can lead to similar appearances to that seen with SIF. Reparative granulation tissue and new bone formation in the necrotic region of ON may demonstrate a similar T2 and enhancement pattern that is seen in SIF [7]. Also, the presence of subchondral linear hyperintensity on fat-suppressed T2W MRI is a common finding in both SIF (93.7%) and advanced

Fig. 2 A 51-year-old woman with sudden onset right hip pain. **a** Anteroposterior (AP) radiograph demonstrates the normal appearance of the right hip. **b** Coronal T1-weighted spin echo (T1W SE) MR image shows a hypointense subchondral band (*arrow*) consistent with a subchondral insufficiency fracture (SIF). **c** Coronal short tau inversion recovery (STIR) MR image shows associated bone marrow oedema (BMO) in the femoral head and neck (*arrow*)

Fig. 3 Differentiation between SIF and osteonecrosis (ON). **a** ON: coronal post-contrast fat-suppressed T1W SE MR image of the left hip in a 14-year-old girl with ON, showing no enhancement of the necrotic fragment (*arrow*). **b** SIF: coronal STIR MR image of the right hip in a 54-year-old man showing a discontinuous subchondral fracture line parallel to the articular surface that has a serpiginous morphology (*arrow*). Note also the extensive BMO. **c** ON: coronal T1W SE MR image of the left hip showing a hypointense line (*arrow*) that is continuous and predominantly concave to the articular surface

ON (79.2%) [30]. With regard to the location of SIFs in the femoral head, they are more prominent in the anterior aspect of the head (Fig. 4) [31]. In one-third of cases, the fracture may be located laterally and contact the acetabular edge (Fig. 5); these patients tend to have a greater degree of acetabular over-coverage. In the remaining patients who have normal acetabular coverage, the fractures are typically located in the centre of the head in the coronal plane (Figs. 2b, 3b) [31]. Follow-up imaging may show either healing of the fracture with reduction of associated BMO, or progression to femoral head collapse.

Owing to ambiguity in the imaging appearances of the two conditions, other clinical factors must be considered. SIF is typically seen in elderly female patients with increased BMI and osteopaenia, and should be considered in the differential diagnosis of any elderly female with acute onset severe hip pain [32]. The presence of concurrent vertebral compression fractures is also predictive of SIF [33]. ON is more commonly seen in younger patients (between 30 and 40 years) with a history of steroid or alcohol use, and is more commonly bilateral [25, 33, 34].

Fig. 4 Sagittal fat-suppressed (FS) T2-weighted fast spin echo (T2W FSE) MR image of the hip showing a SIF (*arrow*) in the anterosuperior aspect of the femoral head, with mixed increased and reduced signal intensity (SI) of the bone above the fracture (*arrowhead*)

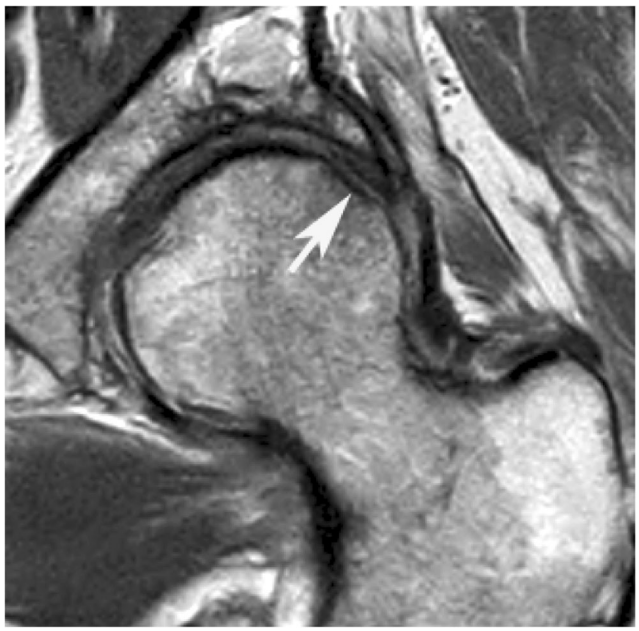

Fig. 5 A 70-year-old woman with left hip pain. Coronal T1W SE MR image showing a laterally located SIF with minor collapse of the femoral head, associated with marked acetabular over-coverage (*arrow*)

Knee

Spontaneous ON of the knee (SONK) was first described in 1968 and thought to be a distinct form of ON unrelated to a systemic disorder or corticosteroid use [35]. The classic secondary ON of the knee is often bilateral, involving large areas of both epiphysis and metaphysis, affecting younger patients and is usually apparent on initial radiographs [35, 36]. On the other hand, SONK was commonly found in elderly patients (average age 70 years), affecting a single joint with propensity for shallow, sub-articular distribution, classically affecting the medial femoral condyle.

Since the recognition of SIF of the hip as a distinct entity, further studies have been carried out to assess the true nature of SONK, with a final diagnosis of SIF being made following histopathological evaluation of surgically managed cases of SONK [37]. A linear fracture line was seen with associated chondral metaplasia, callus formation and granulation tissue. Small foci of ON were present between the fracture and the articular cartilage, but this was not in keeping with what was expected in classical ON of the knee. The surrounding bone was focally resorbed by osteoclastic activity and vascular granulation tissue in keeping with areas of radiolucency on radiographs [37]. Three further histopathological studies have supported the diagnosis of SIF as the cause of SONK, as seen on MRI [38–40]. Therefore, it is now thought that SIF is the primary cause of this MRI appearance, with ON being a likely secondary event to the underlying fracture, and the term SONK should be avoided as a primary diagnosis.

A study of 74 cases of SIF of the knee showed an almost equal distribution between males and females, with a mean age of 61.7 years (range 37–89 years) and 74% presenting in the 6th to 7th decades of life. The mean BMI was 29.9 [41]. A systematic review by Hussain et al. found a correlation between SIF of the knee with patients who had meniscal tear, especially a posterior root tear of the medial meniscus (Fig. 6b). These changes were also found in patients who had undergone meniscectomy and other arthroscopic procedures, including radiofrequency treatment and anterior cruciate ligament (ACL) reconstruction [42]. The most common site for SIF of the knee is at the medial femoral condyle (MFC; Fig. 6). There have been reported cases of SIF involving the lateral femoral condyle (LFC; Fig. 7a), medial and lateral tibial plateau (MTP, LTP), although these are less common [43–46]. Of 74 cases of SIF, the MFC was involved in 64.9%, the LFC and MTP in 16.2% and the LTP in only 2.7% [41].

Patients usually describe sudden onset pain that is out of proportion to the changes evident on radiography [43]. Although the initial radiographs of SIF of the knee are usually normal, follow-up radiographs may demonstrate subchondral bone collapse with focal areas of radiolucency. As with the hip, MRI is the imaging modality of choice. SIF is one of several causes of subchondral BMO in the knee [47]. Classically, MRI demonstrates a discrete area of linear low SI affecting the subchondral bone on T1-weighted imaging (Fig. 7a, b) associated with florid surrounding BMO on T2-weighted and fat-suppressed images (Fig. 7c) [37, 48]. When viewed in the coronal plane, 70% are located centrally (Fig. 7c), 27% peripherally (Fig. 6a) and only 3% at the inner margin of the condyle, whereas on the sagittal images 77% occur centrally (Fig. 6a), 19% posteriorly (Fig. 7b) and only 4% anteriorly. The lesion size can vary from 4 to 31 mm [41]. Associated soft-tissue oedema is seen in 89% of cases, 78% around the medial collateral ligament and 68% posterior to the distal femur. Only 18% have soft-tissue oedema around the tibia, although its presence is highly predictive of SIF of the medial tibial plateau. Joint effusion can be seen in 53% and synovial thickening in 53% [41]. Medial meniscal tears have been reported in 64% of cases, occurring in 73% of MFC SIFs and 21% of LFC SIFs. The tears involved the posterior root in 41% [39]. Progression of SIF to subchondral collapse (Fig. 8) is reported in 68% of cases, this being commoner in female subjects and in patients with meniscal extrusion of 3 mm or more [39].

Early diagnosis and conservative treatment may lead to fracture healing, without progression to subchondral collapse and fragmentation. The initial conservative treatment includes NSAIDs, protected weight-bearing and quadriceps-strengthening. In a small series of patients with SIF, MRI demonstrated a greater reduction in the size of the fracture when treated with the prostaglandin inhibitor iloprost compared with tramadol [49]. If the lesion is less than 3.5 cm^2, patients may do well with conservative management. However, in lesions greater than 5 cm^2 or 40% width of the condyle, prognosis may be unfavourable leading to surgical management [50, 51]. High tibial osteotomy or total knee replacement may be necessary in these cases.

Ankle

Subchondral insufficiency fracture of the talus is rare and can affect both the talar dome (Fig. 9) and the head (Fig. 10), where it articulates with the distal tibia and the navicular respectively [52, 53]. It is hypothesised that compression of the talar head against the navicular during the push-off phase of the normal gait cycle might predispose this segment of the talus to SIF [53]. Similar to other weight-bearing joints, SIF of the talus is thought to occur in post-menopausal women with osteoporosis. MRI demonstrates a linear low SI band along the subchondral region of the talus on T1-weighted imaging (Figs. 9a, 10a), with surrounding high signal representing BMO on T2W and FS imaging (Figs. 9b, 10b). It can be difficult to

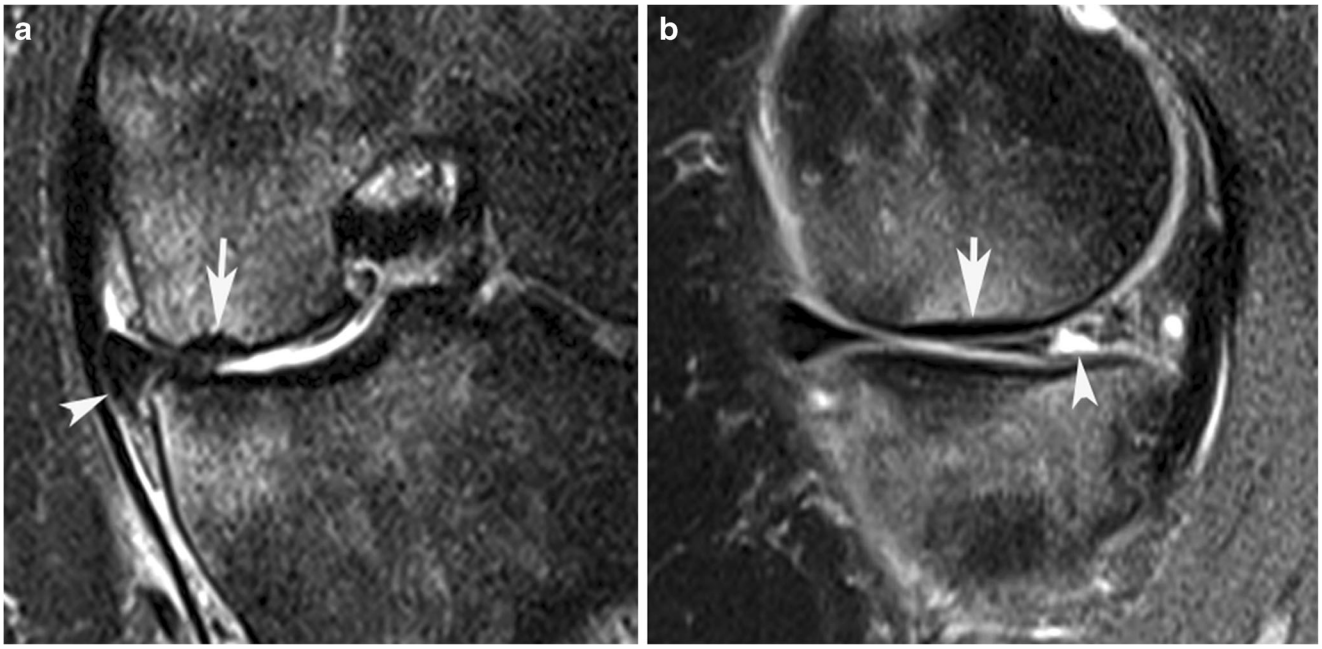

Fig. 6 Subchondral insufficiency fracture of the knee. **a** Coronal STIR MR image of the right knee in a 57-year-old woman showing a peripherally located SIF of the medial femoral condyle (MFC; *arrow*) and extrusion of the meniscal body (*arrowhead*). **b** Sagittal FS T2W FSE MR image showing the SIF (*arrow*) and a posterior third meniscal tear (*arrowhead*)

distinguish SIF from osteochondritis dissecans (OCD) of the talus (Fig. 11). In SIF, there is usually no history of trauma, ligamentous injury or contour deformity and the overlying cartilage remains preserved in the early stages [54]. In contrast, OCD stages 1 and 2 demonstrate articular cartilage injury, commonly involving the medial margin of the talar dome, whereas lateral lesions are almost always associated with a history of trauma [55]. The demographics of the two entities are also different, with SIF affecting the elderly, whereas OCD occurs most commonly in the 2nd decade of life [56].

Metatarsal head

Subchondral insufficiency fracture of the metatarsal (MT) head is difficult to diagnose clinically as it has a similar presentation to other forefoot conditions such as capsulitis, neuroma, metatarsalgia and stress fracture of the metatarsal shaft. Freiberg's infraction was thought to be a cause of metatarsal head collapse in young female subjects, secondary to post-traumatic vascular disruption of the subchondral bone [57]. Repeated microtrauma, systemic disease and biomechanical malalignment are all thought to be contributing factors to

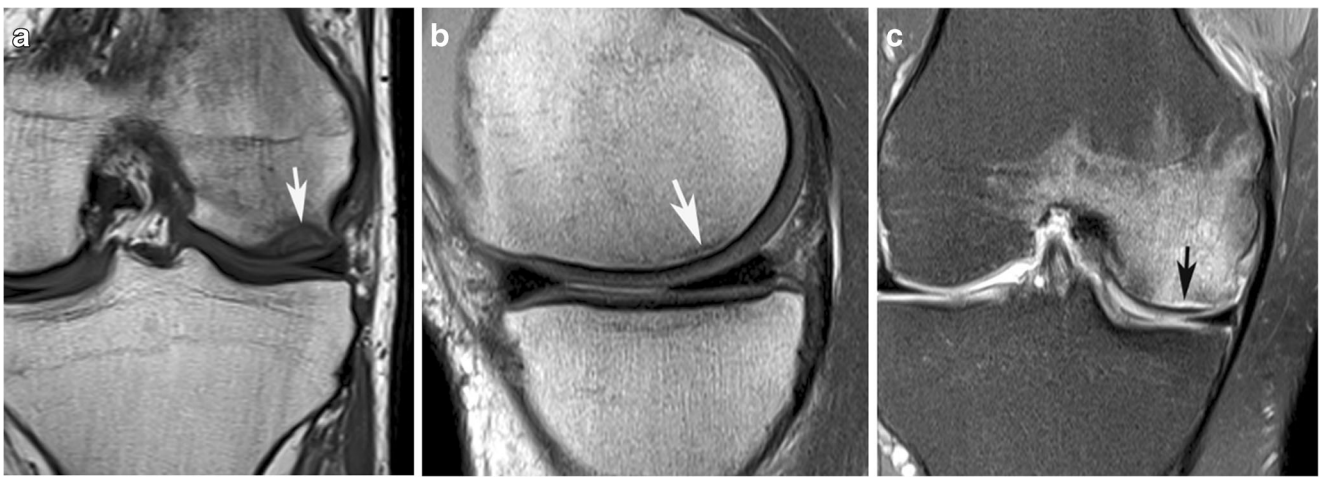

Fig. 7 Subchondral insufficiency fracture of the knee. **a** Coronal T1W SE MR image of the left knee of a 60-year-old man showing a peripherally located SIF of the lateral femoral condyle (*arrow*). **b** Sagittal proton density-weighted (PDW) FSE MR image of the knee of a 56-year-old man showing a posteriorly located SIF of the MFC (*arrow*). **c** Coronal FS PDW FSE MR image of the right knee showing a SIF of the MFC (*arrow*) with prominent associated BMO

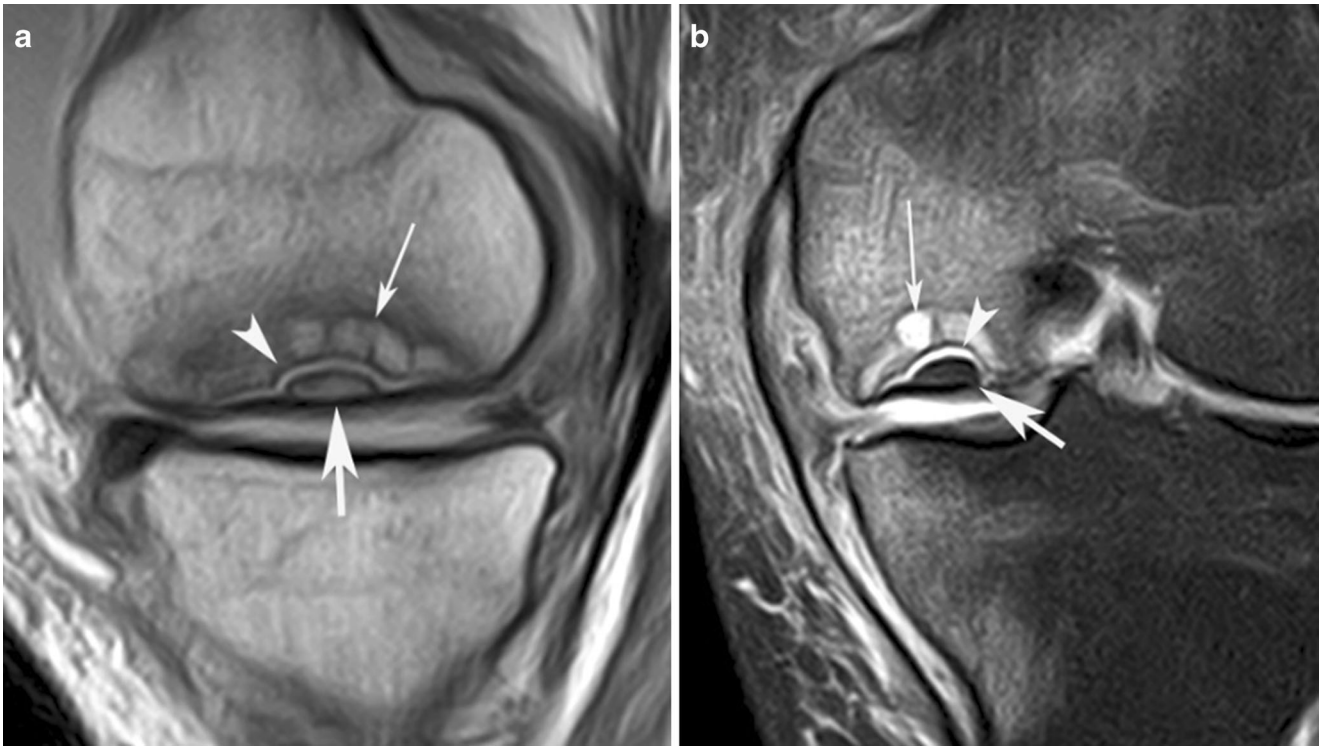

Fig. 8 Subchondral insufficiency fracture of the knee. **a** Sagittal PDW FSE and **b** coronal FS PDW FSE MR images of the right knee of an 83-year-old woman showing mild subchondral collapse with a necrotic fragment (*arrows*) separated from the underlying oedematous bone by a linear fluid SI cleft (*arrowheads*), with associated subchondral cystic change (*thin arrows*)

Freiberg's infraction [58, 59]. Gauthier and Elbaz suggested subchondral fatigue fracture as the initial injury leading to vascular compromise resulting in ON [60]. However, a subsequent study by Young et al. found that non-juvenile

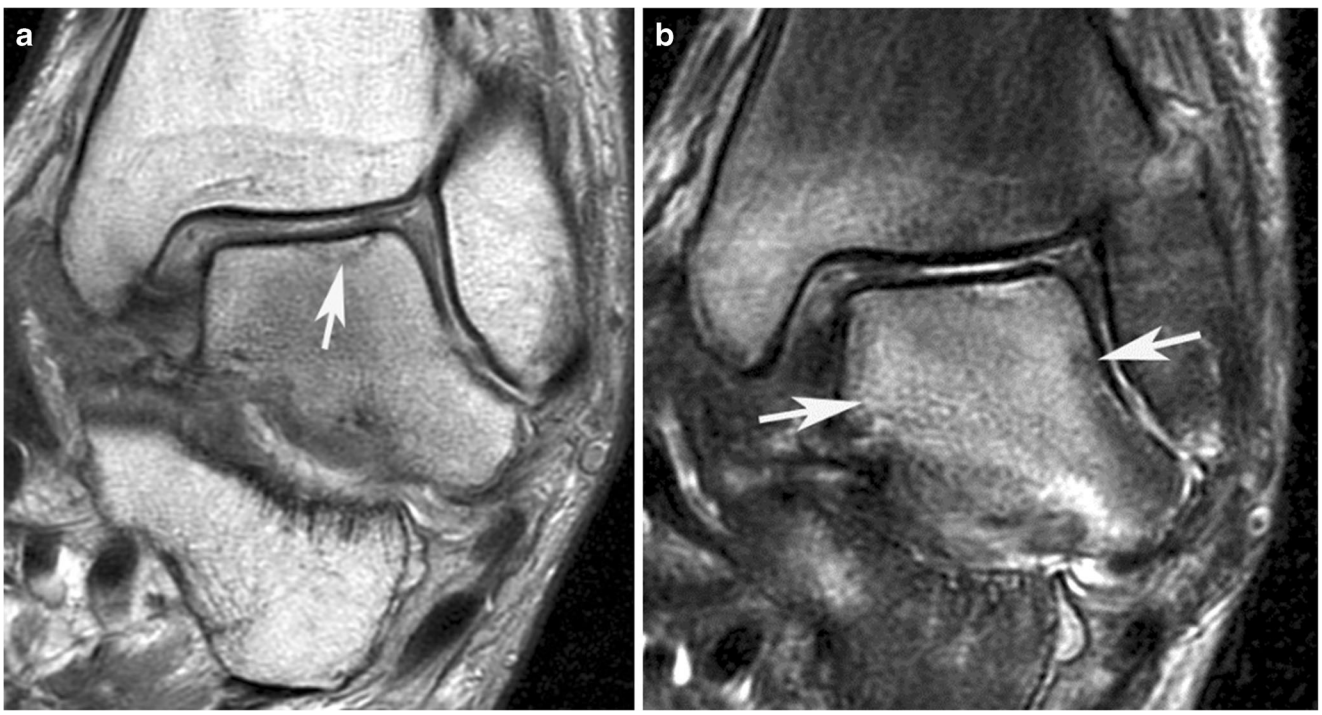

Fig. 9 Subchondral insufficiency fracture of the talar dome. **a** Coronal T1W SE and **b** STIR MR images of a 24-year-old woman with a Charcot joint showing a subtle SIF in the centre of the talar dome (*arrows* in **a**) with extensive associated BMO (*arrows* in **b**)

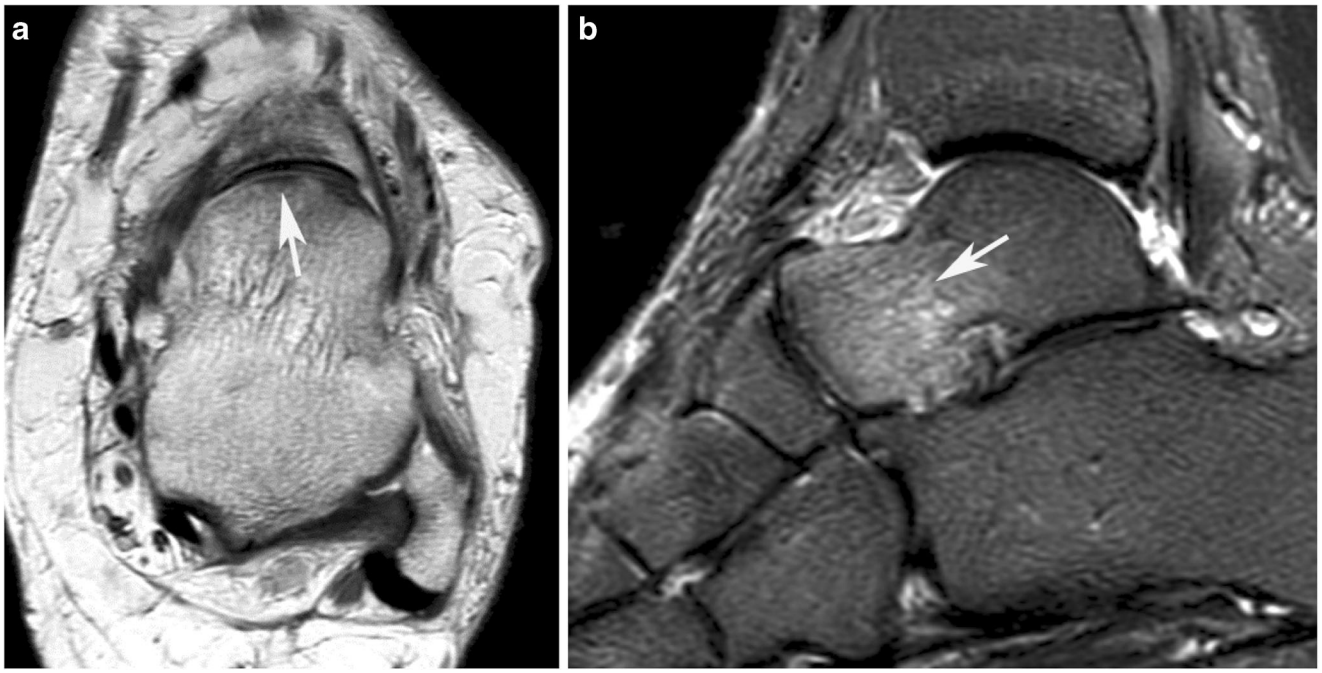

Fig. 10 Subchondral insufficiency fracture of the talar head. **a** Axial T1W SE and **b** sagittal STIR MR images of a 52-year-old woman showing a SIF in the distal articular surface of the talus (*arrow* in **a**) with associated BMO (*arrow* in **b**)

Freiberg's infraction of the MT head is due to osteochondral shearing at the tidemark junction. They hypothesised that during the toe-off phase of the gait cycle, the proximal phalanx might be compressed against the dorsal surface of the MT head causing shearing stresses parallel to the subchondral bone leading to SIF in non-juvenile patients [61]. Histopathological analysis of the MT head in a 77-year old woman with 2nd MT head collapse found granulation tissue with callus formation and vascular supply without any evidence of ON, similar to that seen in SIF of the hips. MRI in this patient demonstrated linear subchondral low SI on T1- and T2-weighted imaging with surrounding bone marrow

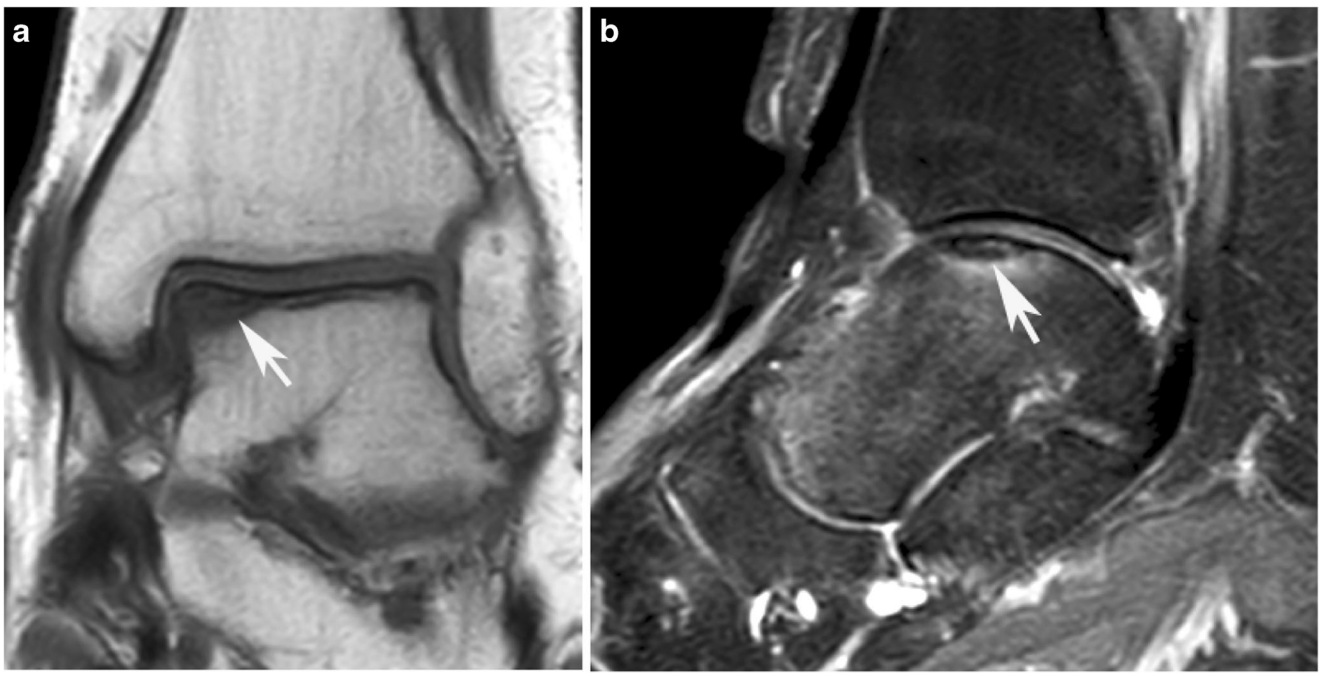

Fig. 11 A 39-year-old woman with left ankle pain. **a** Coronal T1W SE and **b** sagittal STIR MR images showing a subchondral fracture of the medial margin of the talar dome (*arrows*) with little associated oedema. The differential diagnosis lies between a SIF and a stage 2 osteochondral lesion of the talus

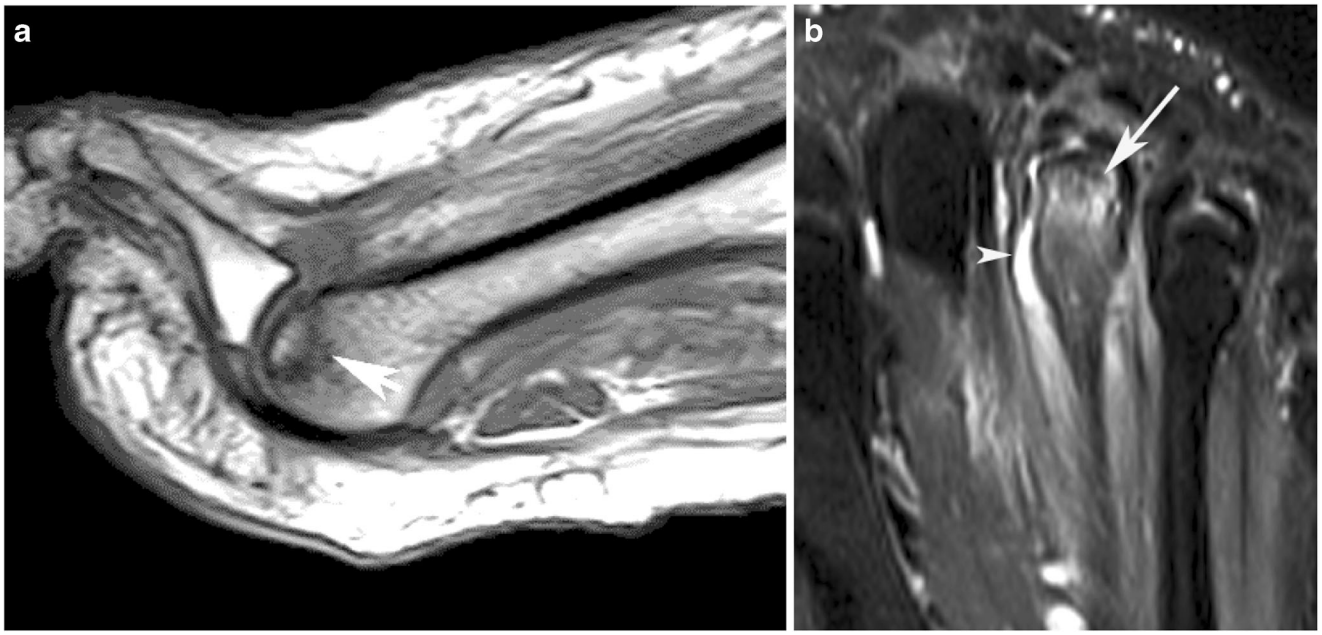

Fig. 12 A 39-year-old woman with right forefoot pain. **a** Sagittal T1W SE MR image showing a SIF in the third metatarsal (MT) head (*arrow*). **b** Axial STIR MR image showing associated BMO (*arrow*) and joint effusion (*arrowhead*)

oedema in keeping with SIF, as seen in other diarthrodial joints [59].

Torriani et al. described the MRI features in 13 patients with 14 MT head SIFs [62]. All patients were women with mean age of 52.8 years (range 25–68.3 years), and a history of acute trauma was reported by 1 patient only. The second MT head was involved in 10 cases, and the third and fourth in 2 cases each. Two MRI patterns were described, the commonest (71%) being a subchondral fracture most frequently involving the dorsal aspect of the MT head (Fig. 12a) with florid oedema-like marrow signal and joint effusion (Fig. 12b). The mean fracture length was 9.5 mm, and flattening of the MT head was observed in 40% of cases. The second pattern comprised subchondral sclerosis with MT head flattening, but little associated marrow oedema (Fig. 13).

Conclusion

Subchondral insufficiency fractures may be difficult to diagnose both clinically and radiologically, and have previously been mislabelled and misdiagnosed as ON. SIF should be considered as a differential diagnosis in the setting of severe non-traumatic joint pain when the initial radiographs appear

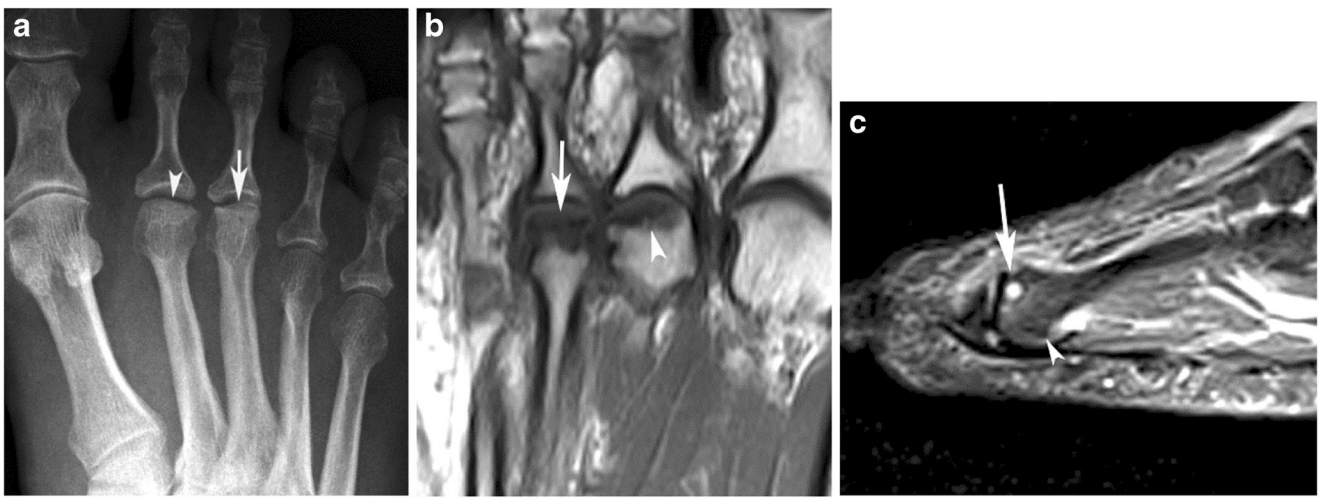

Fig. 13 A 58-year-old woman with a 3-year history of right forefoot pain. **a** Dorsoplantar radiograph showing flattening and sclerosis of the second and third MT heads (*arrows*). **b** Axial T1W SE MR image showing hypointensity in the third MT head (*arrow*) with similar milder changes in the second MT head (*arrowhead*). **c** Sagittal STIR MR image showing associated a flattened third MT head with a subchondral cyst (*arrow*) and no significant BMO (*arrowhead*)

normal. MRI typically demonstrates linear low SI adjacent to the subchondral bone plate with associated florid BMO, especially in elderly patients with a history of osteoporosis or concurrent cartilage and meniscal degeneration. Early conservative management with pain relief and non-weight-bearing is crucial to halt its progression to subchondral bone collapse, which may lead to OA requiring joint replacement.

Compliance with ethical standards

Conflicts of interest The authors declare that they have no conflicts of interest.

Publisher's note Springer Nature remains neutral with regard to jurisdictional claims in published maps and institutional affiliations.

References

1. Bangil M, Soubrier M, Dubost JJ, Rami S, Carcanagues Y, Ristori JM, et al. Subchondral insufficiency fracture of the femoral head. Rev Rhum Engl Ed. 1996;63:859–61.
2. Ikemura S, Yamamoto T, Nakashima Y, Shuto T, Jingushi S, Iwamoto Y. Bilateral subchondral insufficiency fracture of the femoral head after renal transplantation: a case report. Arthritis Rheum. 2005;52:1293–6.
3. Iwasaki K, Yamamoto T, Nakashima Y, Mawatari T, Motomura G, Ikemura S, et al. Subchondral insufficiency fracture of the femoral head after liver transplantation. Skeletal Radiol.2009;38:925–8.
4. Miyanishi K, Hara T, Hamada T, Maekawa M, Tsurusaki S, Morooka T, et al. Co-occurrence of subchondral insufficiency fracture of the femoral head and contralateral femoral neck fracture in a rheumatic patient receiving steroid treatment. Mod Rheumatol. 2008;18:619–22.
5. Depasquale R, Fotiadou A, Kumar DS, Lalam R, Tins B, Tyrrell PNM, et al. Subchondral impaction fractures of the non-weight-bearing portion of the lateral femoral condyle. Skeletal Radiol. 2013;42:177–85.
6. Nelson FR, Craig J, Francois H, Azuh O, Oyetakin-White P, King B. Subchondral insufficiency fractures and spontaneous osteonecrosis of the knee may not be related to osteoporosis. Arch Osteoporos. 2014;9:194.
7. Yamamoto T. Subchondral insufficiency fractures of the femoral head. Clin Orthop Surg. 2012;4:173–80.
8. Gourlay ML, Renner JB, Spang JT, Rubin JE. Subchondral insufficiency fracture of the knee: a non-traumatic injury with prolonged recovery time. BMJ Case Rep. 2015. https://doi.org/10.1136/bcr-2015-209399.
9. Rafii M, Mitnick H, Klug J, Firooznia H. Insufficiency fracture of the femoral head: MR imaging in three patients. AJR Am J Roentgenol. 1997;168:159–63.
10. Song WS, Yoo JJ, Koo K-H, Yoon KS, Kim Y-M, Kim HJ. Subchondral fatigue fracture of the femoral head in military recruits. J Bone Joint Surg Am. 2004;86–A:1917–24.
11. Yamamoto T, Iwamoto Y, Schneider R, Bullough PG. Histopathological prevalence of subchondral insufficiency fracture of the femoral head. Ann Rheum Dis. 2008;67:150–3.
12. Miyanishi K, Hara T, Kaminomachi S, Maeda H, Watanabe H, Torisu T. Contrast-enhanced MR imaging of subchondral insufficiency fracture of the femoral head: a preliminary comparison with that of osteonecrosis of the femoral head. Arch Orthop Trauma Surg. 2009;129:583–9.
13. Viana SL, Machado BB, Mendlovitz PS. MRI of subchondral fractures: a review. Skeletal Radiol. 2014;43:1515–27.
14. Lyons TJ, McClure SF, Stoddart RW, McClure J. The normal human chondro-osseous junctional region: evidence for contact of uncalcified cartilage with subchondral bone and marrow spaces. BMC Musculoskelet Disord. 2006;7:52.
15. Lyons TJ, Stoddart RW, McClure SF, McClure J. The tidemark of the chondro-osseous junction of the normal human knee joint. J Mol Histol. 2005;36:207–15.
16. Oegema TRJ, Carpenter RJ, Hofmeister F, Thompson RCJ. The interaction of the zone of calcified cartilage and subchondral bone in osteoarthritis. Microsc Res Tech. 1997;37:324–32.
17. Madry H, van Dijk CN, Mueller-Gerbl M. The basic science of the subchondral bone. Knee Surg Sports Traumatol Arthrosc.2010;18:419–33.
18. Radin EL, Rose RM. Role of subchondral bone in the initiation and progression of cartilage damage. Clin Orthop Relat Res. 1986(213):34–40.
19. Radin EL, Paul IL. Does cartilage compliance reduce skeletal impact loads? The relative force-attenuating properties of articular cartilage, synovial fluid, periarticular soft tissues and bone. Arthritis Rheum. 1970;13:139–44.
20. Layton MW, Goldstein SA, Goulet RW, Feldkamp LA, Kubinski DJ, Bole GG. Examination of subchondral bone architecture in experimental osteoarthritis by microscopic computed axial tomography. Arthritis Rheum. 1988;31:1400–5.
21. Simon WH. Scale effects in animal joints. II. Thickness and elasticity in the deformability of articular cartilage. Arthritis Rheum. 1971;14:493–502.
22. Shepherd DE, Seedhom BB. Thickness of human articular cartilage in joints of the lower limb. Ann Rheum Dis. England. 1999;58:27–34.
23. Simon WH, Friedenberg S, Richardson S. Joint congruence. A correlation of joint congruence and thickness of articular cartilage in dogs. J Bone Joint Surg Am. 1973;55:1614–20.
24. Yoon PW, Kwak HS, Yoo JJ, Yoon KS, Kim HJ. Subchondral insufficiency fracture of the femoral head in elderly people. J Korean Med Sci 2014;29:593–8.
25. Kubo T, Yamazoe S, Sugano N, Fujioka M, Naruse S, Yoshimura N, et al. Initial MRI findings of non-traumatic osteonecrosis of the femoral head in renal allograft recipients. Magn Reson Imaging. 1997;15:1017–23.
26. Ikemura S, Yamamoto T, Motomura G, Nakashima Y, Mawatari T, Iwamoto Y. MRI evaluation of collapsed femoral heads in patients 60 years old or older: differentiation of subchondral insufficiency fracture from osteonecrosis of the femoral head. AJR Am J Roentgenol. 2010;195:W63–8.
27. Sonoda K, Yamamoto T, Motomura G, Karasuyama K, Kubo Y, Iwamoto Y. Fat-suppressed T2-weighted MRI appearance of subchondral insufficiency fracture of the femoral head. Skeletal Radiol. 2016;45:1515–21.
28. Ikemura S, Mawatari T, Matsui G, Iguchi T, Mitsuyasu H. Clinical outcomes in relation to locations of bone marrow edema lesions in patients with a subchondral insufficiency fracture of the hip: a review of fifteen cases. Br J Radiol. 2016;89:20150750.
29. Yamamoto T, Schneider R, Bullough PG. Subchondral insufficiency fracture of the femoral head: histopathologic correlation with MRI. Skeletal Radiol. 2001;30:247–54.
30. Gondim Teixeira PA, Savi de Tove K-M, Abou Arab W, Raymond A, Louis M, Polet Lefebvre K, et al. Subchondral linear hyperintensity of the femoral head: MR imaging findings and associations with femoro-acetabular joint pathology. Diagn Interv Imaging. 2017;98:245–52.
31. Iwasaki K, Yamamoto T, Motomura G, Karasuyama K, Sonoda K, Kubo Y, et al. Common site of subchondral insufficiency fractures

of the femoral head based on three-dimensional magnetic resonance imaging. Skeletal Radiol. 2016;45:105–13.
32. Yamamoto T, Bullough PG. Subchondral insufficiency fracture of the femoral head: a differential diagnosis in acute onset of coxarthrosis in the elderly. Arthritis Rheum. 1999;42:2719–23.
33. Ikemura S, Yamamoto T, Motomura G, Nakashima Y, Mawatari T, Iwamoto Y. The utility of clinical features for distinguishing subchondral insufficiency fracture from osteonecrosis of the femoral head. Arch Orthop Trauma Surg. 2013;133:1623–7.
34. Fukushima W, Fujioka M, Kubo T, Tamakoshi A, Nagai M, Hirota Y. Nationwide epidemiologic survey of idiopathic osteonecrosis of the femoral head. Clin Orthop Relat Res. 2010;468:2715–24.
35. Ahlbäck S, Bauer GC, Bohne WH. Spontaneous osteonecrosis of the knee. Arthritis Rheum. 1968;11:705–33.
36. Kelman GJ, Williams GW, Colwell CWJ, Walker RH. Steroid-related osteonecrosis of the knee. Two case reports and a literature review. Clin Orthop Relat Res. 1990;(257):171–6.
37. Yamamoto T, Bullough PG. Spontaneous osteonecrosis of the knee: the result of subchondral insufficiency fracture. J Bone Joint Surg Am. 2000;82:858–66.
38. Tanaka Y, Mima H, Yonetani Y, Shiozaki Y, Nakamura N, Horibe S. Histological evaluation of spontaneous osteonecrosis of the medial femoral condyle and short-term clinical results of osteochondral autografting: a case series. Knee. 2009;16:130–5.
39. Mears SC, McCarthy EF, Jones LC, Hungerford DS, Mont MA. Characterization and pathological characteristics of spontaneous osteonecrosis of the knee. Iowa Orthop J. 2009;29:38–42.
40. Higuchi H, Kobayashi Y, Kobayashi A, Hatayama K, Kimura M. Histologic analysis of postmeniscectomy osteonecrosis. Am J Orthop (Belle Mead NJ). 2013;42:220–2.
41. Wilmot AS, Ruutiainen AT, Bakhru PT, Schweitzer ME, Shabshin N. Subchondral insufficiency fracture of the knee: a recognizable associated soft tissue edema pattern and a similar distribution among men and women. Eur J Radiol. 2016;85:2096–103.
42. Hussain ZB, Chahla J, Mandelbaum BR, Gomoll AH, LaPrade RF. The role of meniscal tears in spontaneous osteonecrosis of the knee: a systematic review of suspected etiology and a call to revisit nomenclature. Am J Sports Med. 2017. https://doi.org/10.1177/0363546517743734.
43. Narvaez JA, Narvaez J, De Lama E, Sanchez A. Spontaneous osteonecrosis of the knee associated with tibial plateau and femoral condyle insufficiency stress fracture. Eur Radiol. 2003;13:1843–8.
44. Sokoloff RM, Farooki S, Resnick D. Spontaneous osteonecrosis of the knee associated with ipsilateral tibial plateau stress fracture: report of two patients and review of the literature. Skeletal Radiol. 2001;30:53–6.
45. Ohdera T, Miyagi S, Tokunaga M, Yoshimoto E, Matsuda S, Ikari H. Spontaneous osteonecrosis of the lateral femoral condyle of the knee: a report of 11 cases. Arch Orthop Trauma Surg. 2008;128:825–31.
46. Lotke PA, Nelson CL, Lonner JH. Spontaneous osteonecrosis of the knee: tibial plateaus. Orthop Clin N Am. 2004;35:365–70.
47. Kon E, Ronga M, Filardo G, Farr J, Madry H, Milano G, et al. Bone marrow lesions and subchondral bone pathology of the knee. Knee Surg Sports Traumatol Arthrosc. 2016;24:1797–814.
48. Jose J, Pasquotti G, Smith MK, Gupta A, Lesniak BP, Kaplan LD. Subchondral insufficiency fractures of the knee: review of imaging findings. Acta Radiol. 2015;56:714–9.
49. Mayerhoefer ME, Kramer J, Breitenseher MJ, Norden C, Vakil-Adli A, Hofmann S, et al. MRI-demonstrated outcome of subchondral stress fractures of the knee after treatment with iloprost or tramadol: observations in 14 patients. Clin J Sport Med. 2008;18:358–62.
50. Karim AR, Cherian JJ, Jauregui JJ, Pierce T, Mont MA. Osteonecrosis of the knee: review. Ann Transl Med. 2015;3:6.
51. Aglietti P, Insall JN, Buzzi R, Deschamps G. Idiopathic osteonecrosis of the knee. Aetiology, prognosis and treatment. J Bone Joint Surg Br. 1983;65:588–97.
52. Rios AM, Rosenberg ZS, Bencardino JT, Rodrigo SP, Theran SG. Bone marrow edema patterns in the ankle and hindfoot: distinguishing MRI features. AJR Am J Roentgenol. 2011;197:W720–9.
53. Long NM, Zoga AC, Kier R, Kavanagh EC. Insufficiency and nondisplaced fractures of the talar head: MRI appearances. AJR Am J Roentgenol. 2012;199:W613–7.
54. Roemer FW, Frobell R, Hunter DJ, Crema MD, Fischer W, Bohndorf K, et al. MRI-detected subchondral bone marrow signal alterations of the knee joint: terminology, imaging appearance, relevance and radiological differential diagnosis. Osteoarthritis Cartilage. 2009;17:1115–31.
55. Berndt AL, Harty M. Transchondral fractures (osteochondritis dissecans) of the talus. J Bone Joint Surg Am. 1959;41–A:988–1020.
56. Bruns J, Rosenbach B. Osteochondrosis dissecans of the talus. Comparison of results of surgical treatment in adolescents and adults. Arch Orthop Trauma Surg. 1992;112:23–7.
57. Freiberg AH. Infarction of the second metatarsal bone. Surg Gynecol Obstet. 1914;19:191–3.
58. Brukner P, Bennell K. Stress fractures in female athletes. Diagnosis, management and rehabilitation. Sports Med. 1997;24:419–29.
59. Tsujii M, Hasegawa M, Hirata H, Uchida A. Subchondral insufficiency fracture of the second metatarsal head in an elderly woman treated with autologous osteochondral transplantation. Arch Orthop Trauma Surg. 2008;128:689–93.
60. Gauthier G, Elbaz R. Freiberg's infraction: a subchondral bone fatigue fracture. A new surgical treatment. Clin Orthop Relat Res. 1979;(142):93–5.
61. Young MC, Fornasier VL, Cameron HU. Osteochondral disruption of the second metatarsal: a variant of Freiberg's infraction? Foot Ankle. 1987;8:103–9.
62. Torriani M, Thomas BJ, Bredella MA, Ouellette H. MRI of metatarsal head subchondral fractures in patients with forefoot pain. AJR Am J Roentgenol. 2008;190:570–5.